Taylor & Francis
Taylor & Francis Group

Synthetic Communications

An International Journal for Rapid Communication of Synthetic Organic Chemistry

ISSN: 0039-7911 (Print) 1532-2432 (Online) Journal homepage: https://www.tandfonline.com/loi/lsyc20

Carbon-SO_3H: An efficient catalyst for the synthesis of biscoumarin under ambient reaction conditions and their in silico studies

Ayushi Sethiya, Pankaj Teli, Anu Manhas, Dinesh Agarwal, Jay Soni, Nusrat Sahiba, Prakash Jha & Shikha Agarwal

To cite this article: Ayushi Sethiya, Pankaj Teli, Anu Manhas, Dinesh Agarwal, Jay Soni, Nusrat Sahiba, Prakash Jha & Shikha Agarwal (2020): Carbon-SO_3H: An efficient catalyst for the synthesis of biscoumarin under ambient reaction conditions and their in silico studies, Synthetic Communications, DOI: 10.1080/00397911.2020.1780613

To link to this article: https://doi.org/10.1080/00397911.2020.1780613

SYNTHETIC COMMUNICATIONS®
https://doi.org/10.1080/00397911.2020.1780613

Taylor & Francis
Taylor & Francis Group

Carbon-SO_3H: An efficient catalyst for the synthesis of biscoumarin under ambient reaction conditions and their in silico studies

Ayushi Sethiya[a], Pankaj Teli[a], Anu Manhas[b], Dinesh Agarwal[c], Jay Soni[a], Nusrat Sahiba[a], Prakash Jha[d], and Shikha Agarwal[a]

[a]Synthetic Organic Chemistry Laboratory, Department of Chemistry, Mohan Lal Sukhadia University, Udaipur, India; [b]School of Chemical Sciences, Central University of Gujarat, Gandhinagar, India; [c]Department of Pharmacy, Bhupal Nobel University, Udaipur, India; [d]School of Applied Materials Science, Central University of Gujarat, Gandhinagar, India

ABSTRACT

In this article, we have established a highly promising approach for the synthesis of biscoumarins via domino Knoevenagel–Michael condensation of 4-hydroxycoumarin and aromatic aldehydes in 2:1 ratio using carbon-SO_3H as a solid acid catalyst in H_2O: EtOH (1:1). This new protocol produced α,ά-benzylidene bis(4-hydroxycoumarin) derivatives in high to excellent yields. For this, carbon-SO_3H solid acid catalyst has been prepared from glycerol and sulfuric acid and characterized by FT-IR, SEM, TGA, and X-ray diffraction methods. This approach has several advantages such as high atom-economy (96.05%), excellent yields (88-100%), no need of further purification techniques, that is, column chromatography, easy workup, less reaction time, cost-effective, avoid the use of hazardous solvents, recyclability of catalyst, etc. Moreover, molecular docking studies have been performed on selected proteins methylenetetrahydrohyrofolate reductase (MTHFR) and cytochrome P450 3A4 (CYP3A4) to identify the potency of the synthesized compounds **(3a–j)**. Among the synthesized compounds **3i**, **3e**, and **3b** showed the highest docking score against both the proteins.

GRAPHICAL ABSTRACT

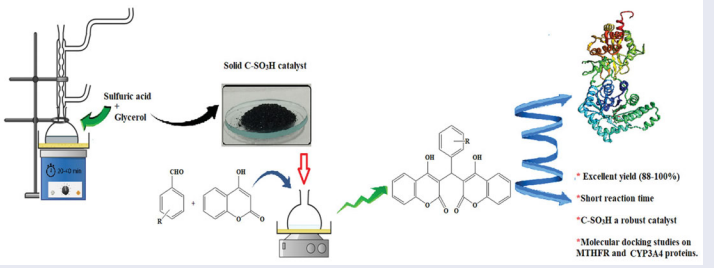

ARTICLE HISTORY

Received 20 March 2020

KEYWORDS

Aldehdyes; biscoumarins; carbon-SO_3H catalyst; click chemistry; 4-hydroxy coumarin; molecular docking

CONTACT Shikha Agarwal shikhaagarwal@mlsu.ac.in Synthetic Organic Chemistry Laboratory, Department of Chemistry, Mohan Lal Sukhadia University, Durga Nursery Road, Udaipur 313001, India.

Supplemental data for this article can be accessed on the publisher's website.

Introduction

The designing of biologically active scaffolds and lead compounds using green protocols by minimizing the pollution and adverse impact on the environment is inevitable.[1] For this, alternative pathways that avoid the use of conventional toxic metal catalysts, solvents, and utilize sustainable and cost-effective sources are indeed required. Therefore, the designing of drugs and its precursors using eco-friendly solvents and catalysts has become one of the most captivating areas in the research field.

Coumarin derivatives are highly valuable scaffolds in the field of synthetic and pharmaceutical chemistry (Fig. 1). It is present in various plants *viz.* tonka bean (*Dipteryx odorata*), sweet woodruff (*Galium odoratum*), etc.[2]

Among coumarin derivatives, biscoumarins are the well-known class of these compounds. These have immense therapeutic applications like anti-coagulant,[3] urease inhibitory,[4] anti-leishmanial,[5] α-glucosidase inhibitor,[6] anti-microbial,[7] enzymatic inhibition activity,[8] HIV integrase,[9] anticancer,[10–12] etc. Instead of numerous pharmacological activities, it showed other applications in the field of organic luminescence material,[13] polymer synthesis,[14] WLED display,[15] and organic semiconductors.[16] Several synthetic pathways have been employed for their synthesis including Knoevenagel, Pechmann, Perkin, Reformatsky, and Wittig reactions. The

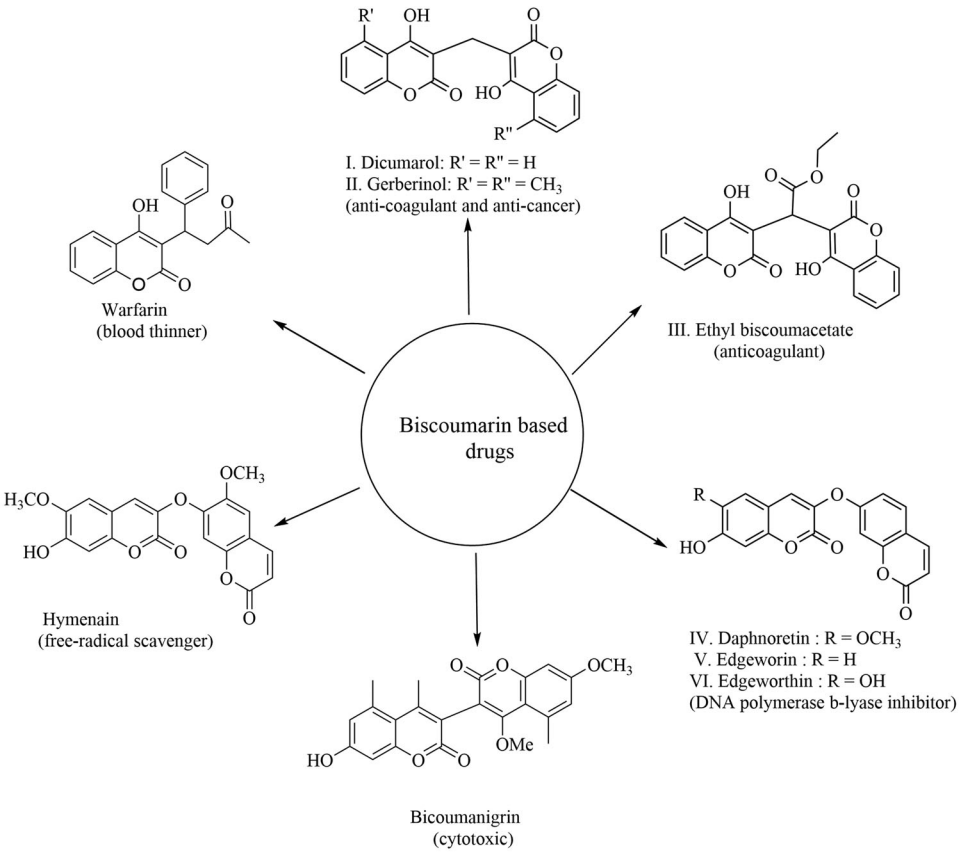

Figure 1. Available drugs possessing biscoumarin scaffold.

Knoevenagel–Michael reaction is also involved in the synthesis of various biologically active scaffolds.[17–19] In the past reports, several methodologies have been designed to prepare biscoumarin derivatives.[20,21] Abramovitch et al. synthesized a series of biscoumarin derivatives using methyl iodide and heating the complex with HCl.[22] Thereafter, several researchers have developed various synthetic methodologies for the synthesis of biscoumarins using heterogeneous catalysts like W-doped ZnO nanocomposites,[23] N-methyl pyrrolidonium zinc chloride,[24] ionic liquid [Dabco-H][AcO],[25] ethylene glycol,[26] zwitterionic liquid (ZIL) coated CuO,[27] o-benzenedisulfonimide,[28] $FeNi_3$-ILs nanoparticles,[29] Fe_3O_4@SiO_2@VB1-Ni(II),[30] ceric ammonium nitrate,[31] taurine,[32] HY-Zeolite,[33] VB_1,[34] choline hydroxide,[35] etc. Several acid catalysts like glacial acetic acid,[36] phosphotungstic acid,[37] pentafluropropanoic acid,[38] phosphor-sulfonic acid,[39] succinimide-N-sulfonic acid[40] other lewis acids like $RuCl_3$,[41] $ZnCl_2$,[42] etc. were also used to improve the selectivity, yield and atom economy. These synthetic pathways have their own merits but include harsh reaction conditions. To overcome these restrictive causes, solid acid catalysts have gained enormous attention due to their surface properties and good acidic characters. In lieu of this, different solid acid catalysts have also been used for biscoumarin synthesis such as sulfonated rice husk,[43] starch–sulfuric acid,[44] silica-bonded n-propyldiethylenetriamine sulfamic acid,[45] cellulose sulfonic acid,[46] melamine trisulphonic acid,[47] Pistachio peels based sulfonic acid.[48] However, the literature-reported pathways have provided efficient access to biscoumarins but include harsh reaction conditions, tedious workup, long reaction time, expensive catalyst, high catalyst loading, limited substrate scope, and use of hazardous solvents. To beat such circumstances and to find a more beneficial protocol, a new eco-friendly method needs to be developed to combat several environmental issues. An exhaustive literature study has been done by our research group[49] and it was found that no work has been done using glycerol-based carbon-SO_3H for the synthesis of biscoumarins to date. Keeping all these points into consideration; we have developed a robust carbon-SO_3H catalyst for the synthesis of biscoumarin derivatives. Carbon-SO_3H has been used earlier to catalyze diverse organic transformations[50–52] and also fruitful for the multi-component reactions to synthesize 4-thiazolidinones, thiazepinones, etc.[53,54] Taking all the points into mind, we have designed a novel approach for the generation of biologically potent biscoumarin derivatives (**3a–j**) using carbon-SO_3H as a robust catalyst. (Scheme 1).

For the molecular docking studies of synthesized compounds (**3a–j**), we have selected cytochrome P450 3A4 (CYP3A4) and methylenetetrahydrohyrofolate reductase (MTHFR) enzyme predicted by PASS online program (PASS online-Way2Drug) (Table 1) and literature studies.[55] PDB IDs pertaining to CYP3A4 and MTHFR are 4D75[56] and 6FCX,[57] respectively. The PASS computer program allows estimating the probable profile of the biological activity of a drug-like organic compound. CYP3A4 catalyzes various oxidative reactions and is recognized as a xenobiotic-metabolizing enzyme in humans.[56] The inhibition of this enzyme is considered beneficial in the treatment of HIV infection.[58] Again, in humans, MTHFR is involved in catalyzing the irreversible reduction of 5,10-methylenetetrahydrofolate to 5-methyl-tetrahydrofolate which is indirectly involved in the biosynthesis of purines and monophosphates.[57] This target is considered essential for the exploration of anti-cancer drugs.[59]

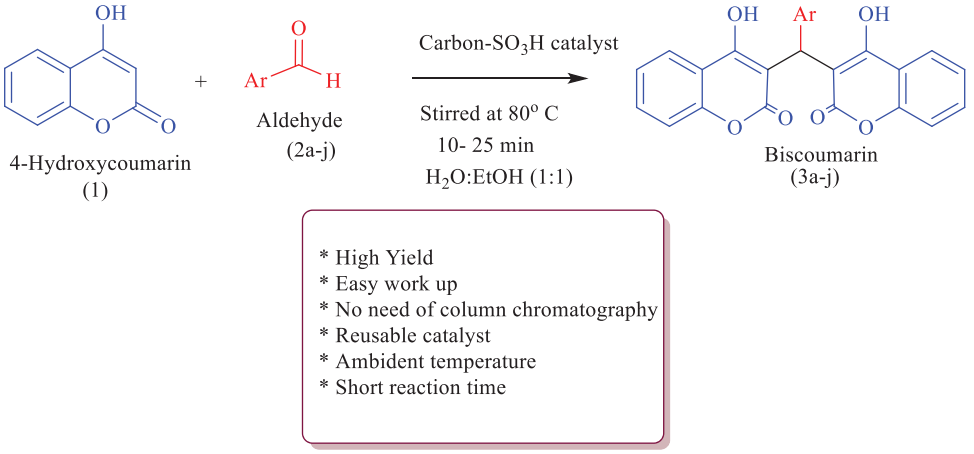

Scheme 1. General reaction for the synthesis of Biscoumarin.

Table 1. Prediction of biological activity by PASS online program for biscoumarin derivatives (Selective).

P_a	P_i	Activity
0.914	0.005	Methylenetetrahydrofolate reductase (NADPH) inhibitor
0.907	0.009	Membrane integrity agonist
0.900	0.004	Aldehyde oxidase inhibitor
0.896	0.004	Monodehydroascorbate reductase (NADH) inhibitor
0.893	0.002	Aryl-alcohol dehydrogenase (NADP+) inhibitor
0.806	0.001	HIV-2 reverse transcriptase inhibitor
0.783	0.003	Antiviral (HIV)
0.799	0.033	Ubiquinol-cytochrome-c reductase inhibitor
0.526	0.046	Platelet adhesion inhibitor
0.426	0.045	Cytochrome P450 stimulant

Note: These types of activities may be revealed by the compound, where $P_a > P_i$ and so they are put into the biological activity spectrum. If $P_a > 0.5$, the compound is likely to reveal its activity in the experiment.

Results and discussion

Chemistry

As a part of our continued interest in catalysis, carbon-SO_3H was found to be an efficient catalyst due to its good catalytic activity, easy recoverability, and reusability up to several runs without loss in the activity. These characteristics have inspired us to establish its viability in the synthesis of biscoumarin derivatives and for further exploration; we prepared carbon-SO_3H catalysts as reported in the literature[60,61] for the synthesis of biscoumarin derivatives. The schematic mechanism for its synthesis and structure has been proposed (Fig. 2).[62,63]

The synthesized catalyst was well characterized by FT-IR, XRD, SEM, and TGA and the results were in accordance with the previously reported papers. As per FT-IR spectra of the carbon-SO_3H catalyst, the two absorption bands at 1146 and 1025 cm^{-1} due to the sulfuric acid group assured the formation of catalysts. The absorption bands appeared at range 3000–3500 cm^{-1} can be endorsed to O–H stretching vibrations (including SO_3H, COOH, and adsorbed water). The peak at 3737 cm^{-1} is due to

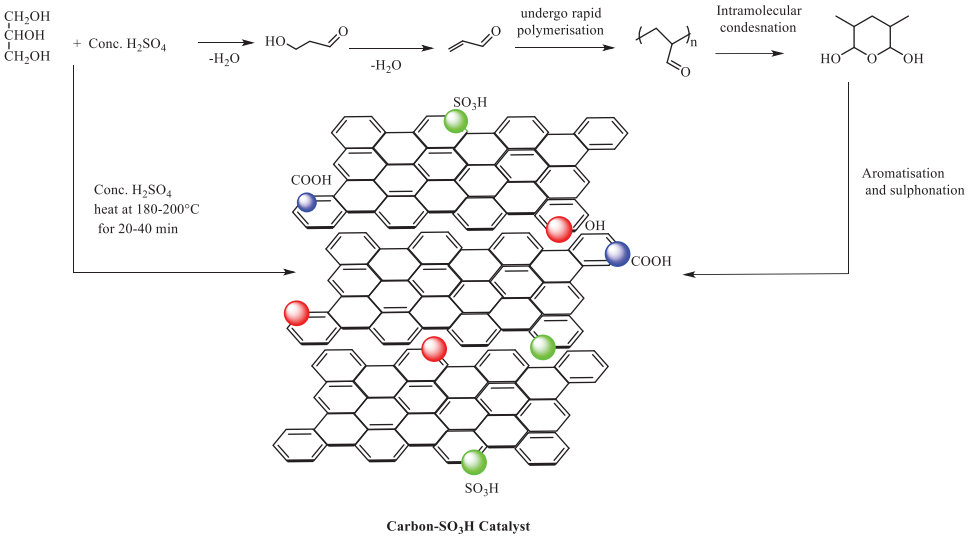

Figure 2. Proposed Schematic mechanism for the carbonization of glycerol by conc. sulfuric acid.

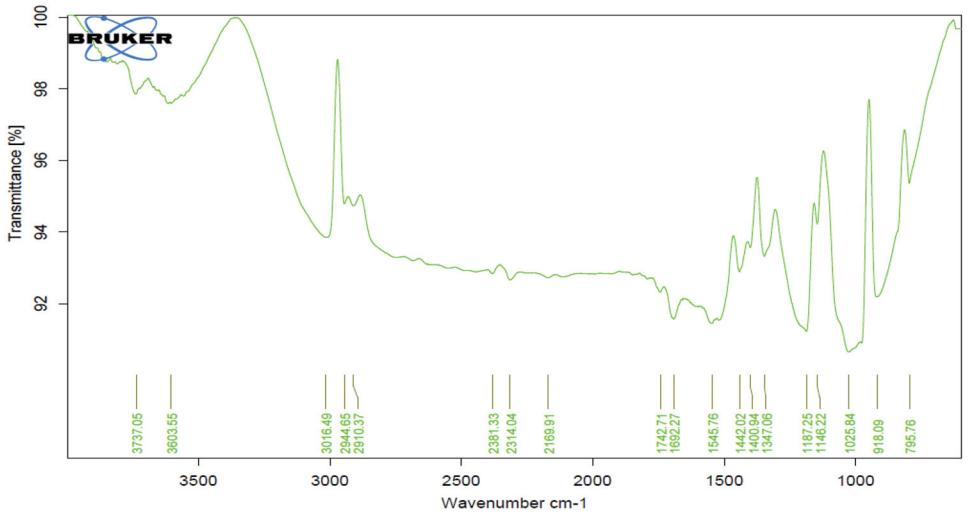

Figure 3. IR spectrum of synthesized carbon-SO_3H.

adsorbed water and at 3603 cm^{-1} is due to OH group of COOH group, 3016 cm^{-1} is related to bonded OH of SO_3H group. The absorption band at 1742 cm^{-1} is related to the carbonyl functional group (Fig. 3). All these absorption peaks were in good agreement with the previously synthesized C-SO_3H catalyst as per Devi et al.[60] In X-ray diffraction (XRD) diffraction peaks at $2\theta = 15–30°$ and $2\theta = 40–50°$ recognized amorphous structure of carbon (Fig. 4).[60] The morphology of the sample was investigated with the scanning electron microscopy (SEM), which showed the agglomerate structure of particles (Fig. 5). The thermal stability of the catalyst was evaluated using the thermogravimetric analysis and the results are shown in (Fig. 6).[60] Thermal degradation patterns depend on the dehydration temperature, which affects both the number of carbon

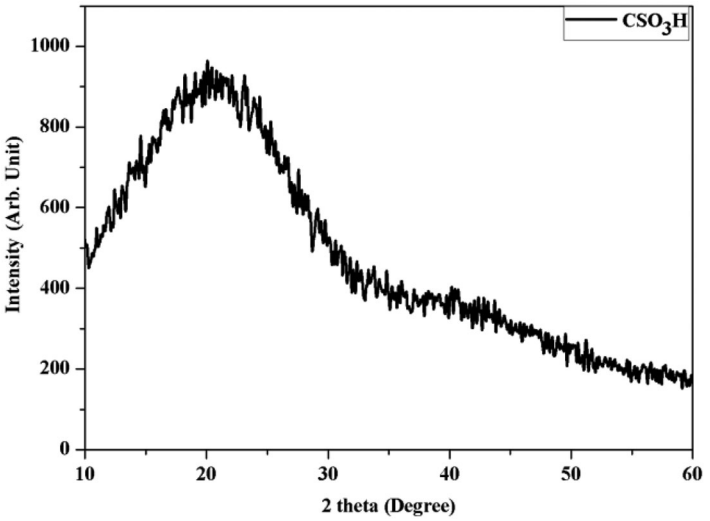

Figure 4. XRD pattern of synthesized carbon-SO_3H.

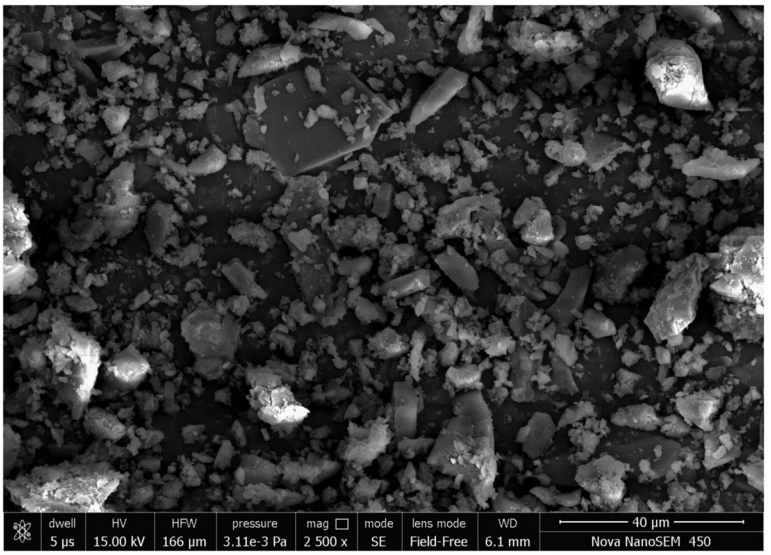

Figure 5. SEM images of synthesized carbon-SO_3H catalyst.

functional groups present and the degree of carbonization. The catalyst showed an initial mass loss due to adsorbed water. A second mass loss was seen at 150–200 °C, most likely due to the loss of SO_3H groups[64,65] TGA analysis showed that the catalyst was stable to 300 °C.[62]

To examine the catalytic efficiency of carbon-SO_3H catalyst, the reaction of 4-OH Coumarin **1** (5 mmol) and 4-Cl benzaldehyde (2.5 mmol) **2a** was taken as the model reaction. For this, the reactants were taken in 50 mL round-bottomed flask with 10 mg of catalyst in solvent-free conditions and stirred at room temperature for an appropriate time (Table 2, Entry 2). The progression of the reaction was monitored by TLC and it took 60 min for the completion of the reaction and a 75% yield was obtained. Parallel

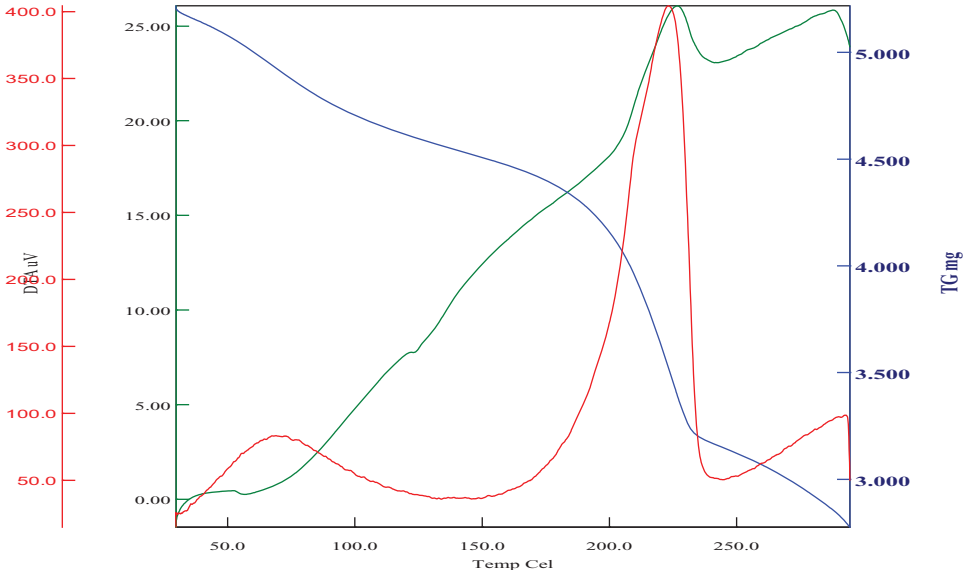

Figure 6. TGA and DTA curve of synthesized carbon-SO_3H catalyst.

Table 2. Typical optimization of the solvent for the preparation of bis(4-hydroxycoumarin) derivatives.

Entry	Catalyst (mg)	Solvent	Temperature	Time (min)	Yield
1		Solvent-free	RT	240	No reaction (%)
2	10	Solvent-free	RT	60	75[b]
3	20	Solvent -free	RT	60	80[b]
4	20	H_2O	RT	60	75[a]
5	20	EtOH	RT	60	72[a]
6	20	H_2O:EtOH (1:1)	RT	60	85[b]

Reaction conditions: 4-Cl benzaldehyde (2.5 mmol), 4-OH coumarin (5 mmol).
[a]The reaction was not completed.
[b]The yields are related to the isolated products.

Table 3. Optimization of catalyst concentration and temperature.

Entry	Catalyst (mg)	Solvent	Temperature	Time (min)	Yield (%)
1	25	H_2O:EtOH (1:1)	RT	35	88[a]
2	30	H_2O:EtOH (1:1)	RT	30	90[a]
3	35	H_2O:EtOH (1:1)	RT	30	90[a]
4	20	H_2O:EtOH (1:1)	80 °C	20	90[a]
5	25	H_2O:EtOH (1:1)	80 °C	20	94[a]
6	30	H_2O:EtOH (1:1)	80 °C	20	100[a]
7	35	H_2O:EtOH (1:1)	80 °C	20	100[a]

Reaction conditions: 4-Cl benzaldehyde (2.5 mmol), 4-OH coumarin (5 mmol).
[a]The yields are related to the isolated products.

to this, the same reaction was performed with 20 mg of catalyst and gave an 80% yield (Table 2, Entry 3). Then, we optimized the reaction conditions by varying solvents and performed the reaction in the water at room temp. (Table 2, Entry 4) and 75% yield was obtained. Simultaneously, the reaction was carried out in ethanol and H_2O:EtOH (1:1) with 20 mg of catalyst (Table 2, Entry 5, 6). It was noteworthy that the high yields were obtained in H_2O:EtOH (1:1).

Table 4 Synthesis of bis(4-hydroxycoumarin) derivatives in the presence of carbon-SO_3H as the catalyst.

Entry	Aldehyde	Symbol for product	Time (min)	Yield (%)
1	4-Cl·C_6H_4	**3a**	20 min	100
2	4-OH·C_6H_4	**3b**	22 min	95
3	4-CN·C_6H_4	**3c**	25 min	91
4	4-F·C_6H_4	**3d**	20 min	92
5	4-NO_2·C_6H_4	**3e**	20 min	94
6	3-OCH_3·C_6H_4	**3f**	10 min	95
7	2-Thiophene	**3g**	15 min	88
8	4-NMe_2·C_6H_4	**3h**	15 min	96
9	1-Naphthyl	**3i**	25 min	89
10	4-OC_2H_5·C_6H_4	**3j**	20 min	95

Table 5. Comparative study on the present method with the reported methods.

S no.	Catalyst	Catalyst loading	Solvent	Condition	Time	Yield (%)	Ref.
1.	Catalyst-free		H_2O	Microwave irradiation at 150 W and 150 °C	8–10 min	76–94	[66]
2.	Glacial acetic acid or Ethanol			Reflux	6 h	65–78	[36]
3.	Phospho tungstic acid	15 mol%	H_2O	Heat 80 °C	14–25 min	90–98	[37]
4.	Pentafluropropanoic acid	40 mol%	H_2O	Reflux	60–100 min	86–92	[38]
5.	Phospho sulfonic acid	50 mg	Solvent-free	Heat 100 °C	15–90 min	63–93	[39]
6.	$RuCl_3$	5 mol%	H_2O	Heat 80 °C	25–35 min	75–95	[41]
7.	$ZnCl_2$	15 mol%	Solvent-free	110 °C	35 min	85–90	[42]
8.	Sulfonated rice husk	40 mg	H_2O	Heated at 80 °C	10–70 min	87–95	[43]
9.	Cellulose sulfonic acid	20 mg	H_2O	Reflux	100–150 min	80–90	[46]
10.	Carbon-based solid acid from pistachio peel	50 mg		Stirred at 80 °C	3–20 min	85–95	[48]
11.	Ceric Ammonium Nitrate	10 mol %	H_2O	RT, Stirring	360–480 min	75–98	[31]
12.	Taurine	0.20 mmol	H_2O	Reflux	35–85 min	84–96	[32]
13.	Zeolite-HY		EtOH	Reflux	60–180 min	80–96	[33]
14.	Fe_3O_4@SiO_2@VB1-Ni^{II}	10 mg	Solvent-free	110 °C	30–50 min	78–98	[30]
15.	ZIL@CuO	0.5 mol%	Solvent-free	Mechanical ball mining with speed of 600 rpm	180 min	90–95	[27]
16.	N-methyl pyrrolidonium zinc chloride	20 mg	Solvent-free	Reflux with stirring	30–50 min	78–97	[24]
17.			Ethylene glycol	90 °C	1.5–3 h	82–92	[26]
18.	o-Benzenedi sulfonimide	50 mol%	H_2O	Reflux	25–30 min	74–91	[28]
19.	VB_1	1 mol%	H_2O/solvent free	RT	180–600 min	82–94	[34]
20.	Carbon-SO_3H	30 mg	H_2O:EtOH (1:1)	Stirring at 80 °C	10–25 min	88–100	Present work

To expedite the reaction, the amount of catalyst was successively increased (Table 3). With an increase in the amount of catalyst, the product yield increased and reaction time decreased. The reaction temperature was also optimized (Table 3, Entry 4-6). The best results were obtained in H_2O:EtOH (1:1) by stirring at 80 °C with 30 mg of catalyst and 100% yield was obtained. (Table 3, Entry 6). Further increase in the catalyst concentration did not affect the reaction time.

In order to investigate the synthetic utility and the scope of the reaction, a series of aryl aldehydes having electron-withdrawing and electron-donating groups as well as heteroaryl derivatives were scrutinized. All aldehydes gave high yields irrespective of the nature of the substituents as summarized in (Table 4).

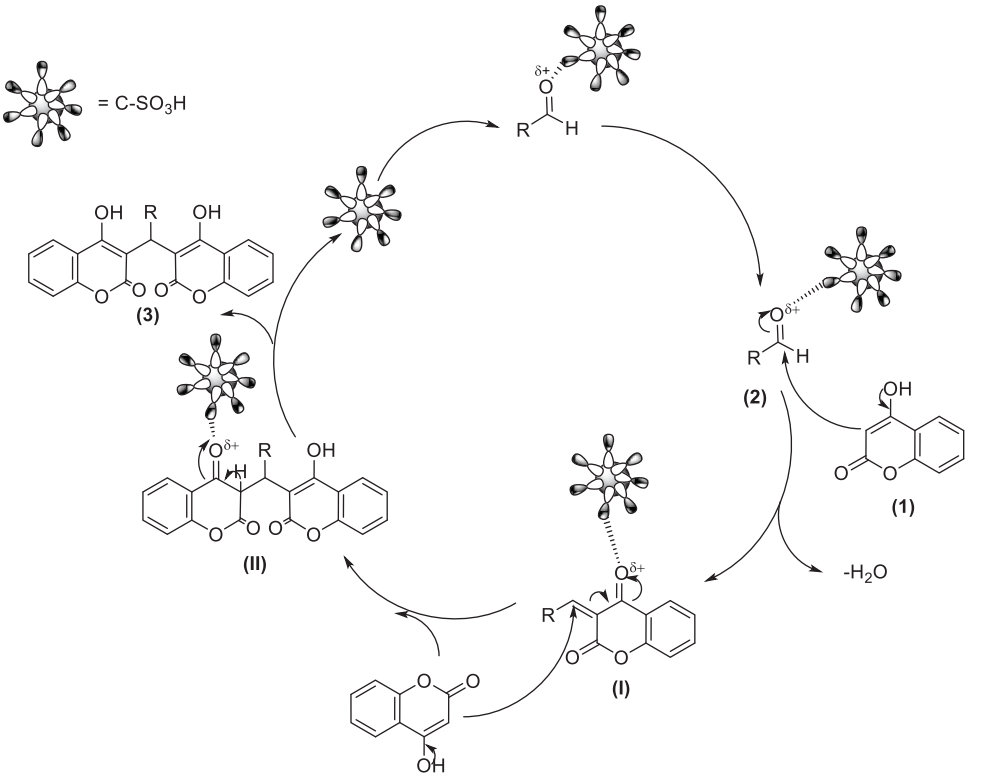

Scheme 2. Putative mechanism for carbon-SO_3H catalyzed synthesis of biscoumarin derivatives.

The appropriateness of this process was determined by comparing the model reaction with the previously reported protocols (Table 5).

Although some of the previously reported methods took less time as compared to Carbon-SO_3H catalyst they suffer from low yields and involve toxic and costly reagents for the synthesis of catalyst, tedious work-up, and harsh reaction conditions. Whereas the present work has several benefits like reusability and recyclability of catalyst, cost-efficient pathway, avoids the use of hazardous solvents with excellent yields, high atom economy, and high E-factor in a short period of time. The structures of all the synthesized compounds (**3a-j**) were corroborated by FT-IR, ^{1}H NMR, ^{13}C NMR, Mass spectrometry, and elemental analysis. The FT-IR spectrum showed a broad absorption at 3058 cm^{-1} due to OH stretching frequency. The vibrational modes of C=O and C–O groups appeared at 1695–1440 and 1350 cm^{-1}, respectively. In addition, the resonating signal at δ 8–11 ppm was attributed to the OH proton in ^{1}H NMR spectra. But OH resonating signals of some compounds were broadened or disappeared due to the interaction with the aqueous DMSO-d_6 as a polar and hydrogen bond acceptor solvent. The methine proton became visible as a singlet near to δ 6.7–5.5 ppm. Additionally, in the ^{13}C NMR spectra, the signals at δ 166.26–162.21 and δ 35.72–31.44 ppm corresponded to carbonyl and methine carbon atoms.

The putative mechanism for the formation of biscoumarin derivatives was elaborated in Scheme 2. The carbon-SO_3H enhanced the electrophilic character of carbonyl carbon of aldehyde. It underwent Knoevenagel condensation with one molecule of 4-

Table 6. Docking scores of the selected hits with the 6FCX protein.

Molecules	Docking score[a]	Match score[a]	Lipo score[a]	Ambig. score[a]	Clash score[a]	Rot score[a]	Match[b]
3i	−26.37	−24.30	−11.04	−07.79	4.36	7.00	35
3e	−25.41	−24.39	−09.68	−10.48	6.73	7.00	25
3f	−24.01	−23.48	−13.45	−11.22	10.33	8.40	24
3b	−23.93	−23.74	−11.28	−06.29	3.58	8.40	28
3g	−22.11	−22.11	−18.07	−12.39	−9.90	7.00	21
3j	−21.72	−25.14	−12.02	−08.31	8.55	9.80	24
3h	−21.15	−21.64	−11.19	−09.42	8.71	7.00	25
3a	−20.76	−21.34	−10.25	−08.74	7.18	7.00	24
3c	−20.70	−21.07	−14.13	−09.80	11.91	7.00	20
3d	−20.69	−18.77	−12.97	−09.44	8.10	7.00	25

[a]kJ/mol.
[b]number of matches.
Match score: contribution of interacting groups; Lipo score: lipophilic-contact area contribution; Ambig score: lipophilic-hydrophilic ambiguous contact area; Clash score: clash penalty contribution; Rot score: entropy contribution of ligand conformation.

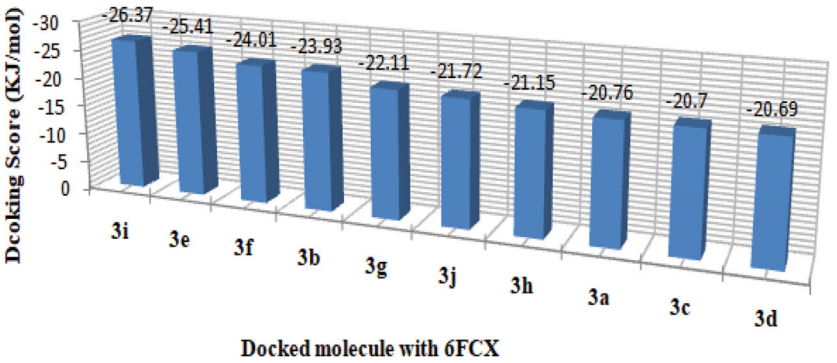

Figure 7. Graphical representation of the docked molecules (**3a–j**) within the binding pocket of 6FCX protein.

hydroxycoumarin to furnish intermediate I, followed by the Michael addition with the second molecule of 4-hydroxycoumarin and formed the desired product.

Docking assessment

Protein 6FCX

From the docking result of 6FCX, it was observed that all the synthesized compounds **(3a-j)** showed binding with the 6FCX protein (Table 6). From Table 6, it was concluded that **3i** showed the highest docking score of −26.37 kJ/mol followed by **3e, 3f, 3b,** and **3g** (Fig. 7). Further, on considering the 3D orientation of the docked molecules, All molecules were docked within the same pocket of the protein (Fig. 7; Docked structures of other compounds are provided in SI).

On analyzing the 2D and 3D interaction plots (Fig. 8) of the docked compounds, it was observed that almost in all molecules, greater than 3 H-bonding interactions were reported with the interaction with amino acid Tyr197 and His201 being the common one. Moreover, the number of other H-bonding and hydrophobic interactions were also witnessed as shown in Figure 7. Therefore, based on the docking score and population

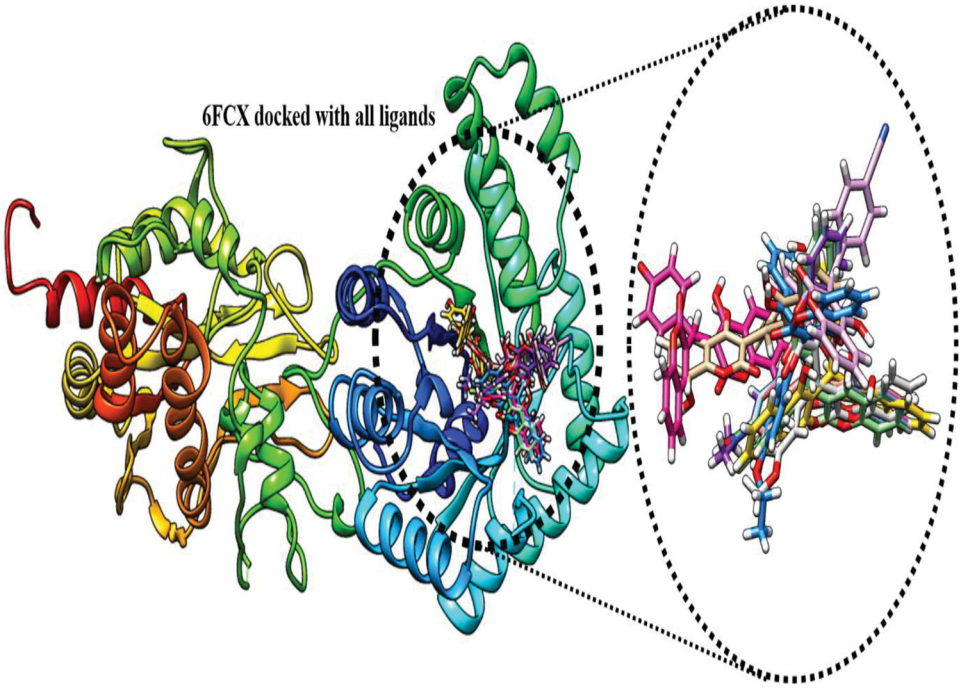

Figure 8. Pictorial representation of all the ligands docked within the same active site of 6FCX protein.

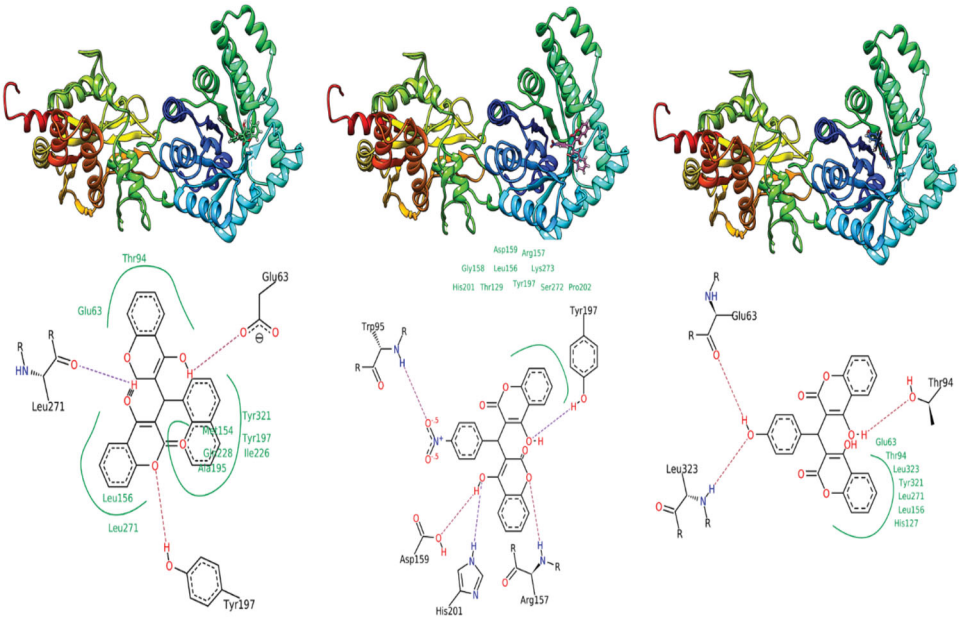

Figure 9. The 2D/3D interaction of highest docked molecules **3i**, **3e**, **3b**.

Table 7. Docking scores of the selected hits with 4D75 protein.

Molecules	Docking score[a]	Match score[a]	Lipo score[a]	Ambig. score[a]	Clash score[a]	Rot score[a]	Match[b]
3i	−13.85	−10.42	−16.05	−5.83	06.06	7.00	29
3e	−11.56	−13.03	−11.49	−6.77	07.34	7.00	18
3b	−09.53	−16.33	−08.47	−5.81	07.29	8.40	22
3h	−08.00	−09.65	−11.50	−4.65	05.40	7.00	25
3d	−05.02	−07.90	−102.56	−4.23	07.27	7.00	22
3a	−01.32	−07.84	−11.76	−4.01	09.89	7.00	24
3j	06.86	−06.81	−12.07	−6.68	17.22	9.80	17

[a]kJ/mol.
[b]number of matches.
Match score: contribution of interacting groups; Lipo score: lipophilic-contact area contribution; Ambig score: lipophilic-hydrophilic ambiguous contact area; Clash score: clash penalty contribution; Rot score: entropy contribution of ligand conformation.

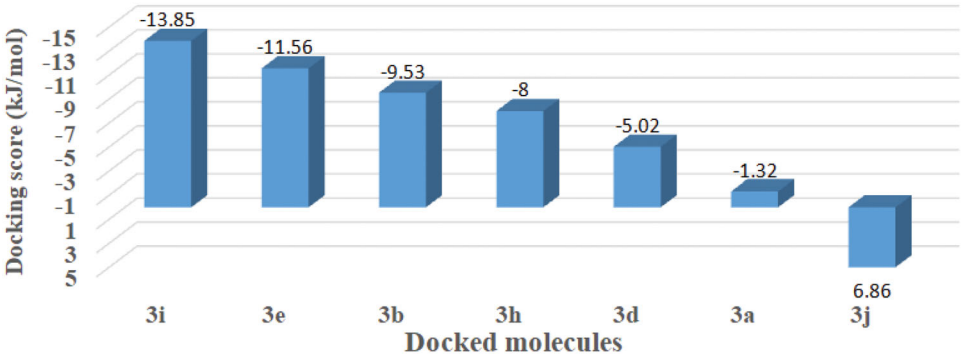

Figure 10. Graphical representation of the seven active docked molecules within the binding pocket of 4D75 protein.

of the docked compounds, compounds **3i, 3e, 3f, 3b, 3g,** and **3j** can be considered as potent molecules for inhibiting the activity of the enzyme (Fig. 9).

Protein 4D75

After conducting docking on 4D75, it was observed that out of 10 molecules, only 7 were able to bind in the active site of the respective protein (Table 7). It is clearly evident from Table 7, that **3i** showed the highest docking score of −13.85 kJ/mol followed by **3e, 3b, 3h, 3d,** and **3a** (Fig. 10). On observing the 3D orientation of the docked molecules, it was obvious that all the molecules bound well within the same pocket (Fig. 10).

From the generated 2D and 3D interaction plots, it was observed that among the synthesized molecules **3i, 3e,** and **3j** showed H-bonding interaction with the amino acid Arg 212, which is considered important for the inhibition of the enzyme[56] (Fig. 11). Besides, in **3d** and **3a,** the interaction with Arg212 was seen in the hydrophobic form. Moreover, among all the molecules, a common hydrophobic interaction was observed with Arg105 and Hem 601, which was also documented as the crucial interaction.[56] Thus, we can conclude that based on the docking score and presence of crucial interactions, **3e, 3i,** and **3b** can be considered as the potent inhibitors of CYP3A4 protein (Fig. 12; The docked structure of the other compounds in SI).

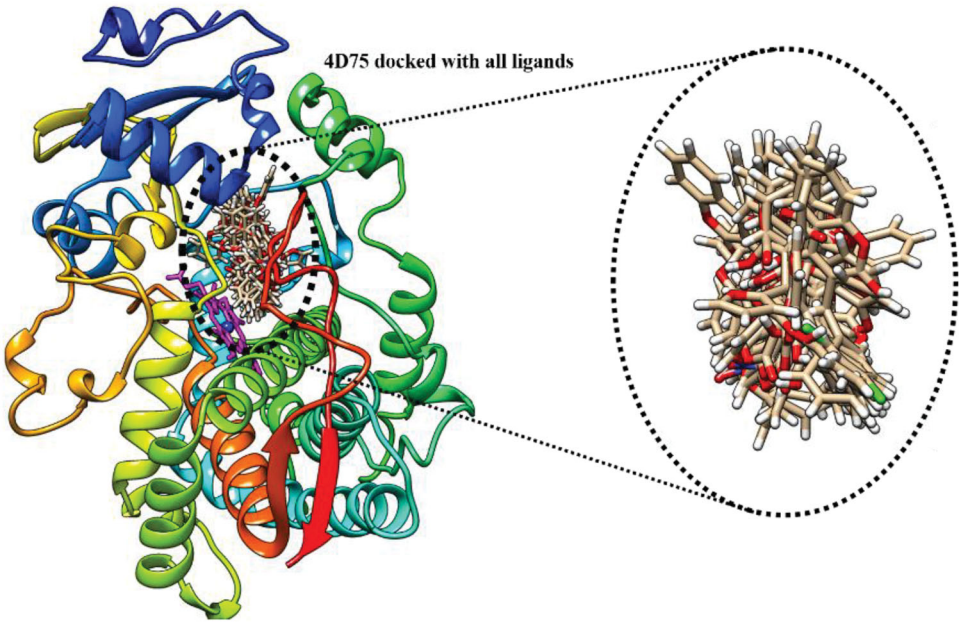

Figure 11. Pictorial representation of all the ligands docked within the same active site of 4D75 protein.

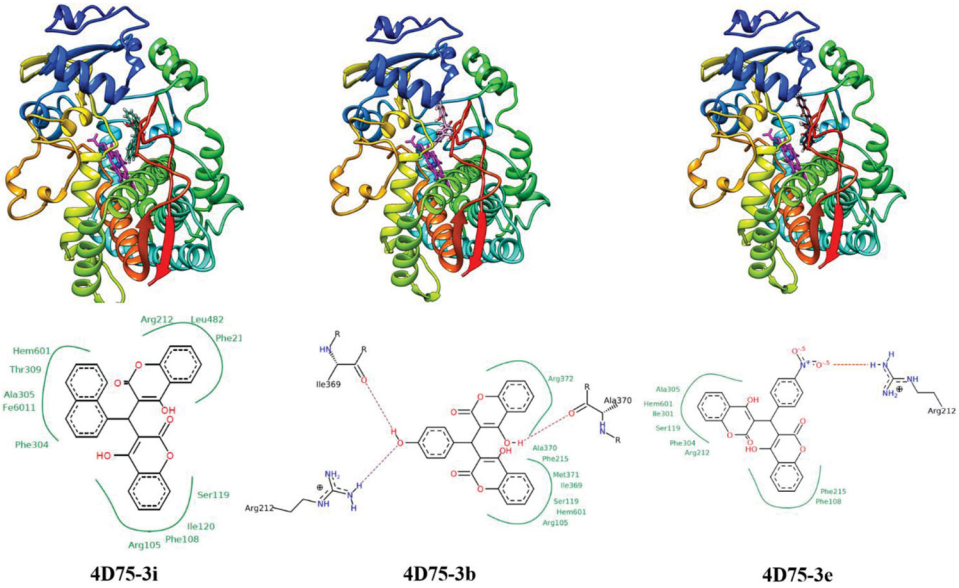

Figure 12. 2D and 3D interaction plots of the docked **3i**, **3e**, and **3b** ligands within the binding pocket of 4D75 protein.

Green chemistry matrices for a reaction

When green chemistry matrix[67,68] was calculated, it was found that the reaction has low environment-factor (E-factor = 0.0421), high atom economy (AE = 96.05%),

process mass intensity (PMI = 1.74) and reaction mass efficiency (RME = 95.9%), with excellent eco-score (90) as shown in SI. These values clearly specified the eco-friendly nature of the present technique.

Conclusions

In this study, carbon-SO_3H being a heterogeneous and recyclable robust catalyst was found to be very efficient for the production of biscoumarin derivatives by a click chemistry approach. The protocol is facile and environmentally benign as it doesn't involve any solvent, high atom economy, and no by-products are generated. The excellent yields (88–100%) under mild reaction conditions in just 10–25 min made this protocol a user-friendly approach for the synthesis of biscoumarins. The synthesis of the catalyst was very simple and easily recovered and reused for successive cycles. The docking studies were also performed in order to enhance its biological profile. In the future, this carbon-SO_3H shall be used for many multi-component reactions and for the high throughput screening in medicinal chemistry. From the docking outcome of both calculations, it can be concluded that commonly **3e** and **3b** form stable binding interactions with CYP3A4 and MTHFR enzymes. In the case of both enzymes, the docked compounds are able to form crucial H-bonding and other hydrophobic interactions. Thus, we may consider these compounds (**3i, 3e, 3b**) may show inhibitory activity against the selected proteins.

Experimental

All chemicals were procured from Sigma-Aldrich, Spectrochem, Loba-Chemie and used without further purification. Melting points were determined in open capillary tubes and were uncorrected. The IR spectra were recorded in KBr pellets on a Bruker FT-IR spectrometer. The ^{1}H NMR (500 MHz) and ^{13}C NMR (500 MHz) spectra of synthesized derivatives were scanned on a Bruker Avance NEO 500 MHz spectrometer using tetramethylsilane (TMS) as an internal standard and DMSO as a solvent. The mass spectra were recorded on a Waters Xevo G2-S QT spectrometer. XRD analysis was done by X-Ray diffractometer (Rikagu Miniflex) and SEM was performed on Nova nano SEM 450. The TG/DTA analysis was done by TG/DTA7300 of EXSTAR. The purity of derivatives was examined by thin-layer chromatography (TLC) eluting with hexane:ethylacetate in (1:1) ratio.

General procedure for the synthesis of glycerol-based carbon sulfonic acid catalyst

The glycerol-based carbon sulfonic acid catalyst was synthesized by taking a mixture of glycerol (20 g) and concentrated sulfuric acid (80 g) and was gently heated on a sand bath in a temperature range of 180–200 °C for 20–30 min, to assist *in situ* partial carbonization and sulfonation. The mixture was kept at that temperature for about 40 min (until foaming ceased) to get the polycyclic aromatic carbon compound. The crude product was allowed to kept at normal temperature and treated with hot distilled water under agitation till the decant water neutralized and pH became 7. The partially crystalline black color product was

filtered and dried in an oven at 120 °C for 2–3 h until it was free from moisture. The weight of the dried catalyst was found to be 9.22 gm.[60,61]

General procedure for the synthesis of biscoumarin derivatives

To synthesize biscoumarin, a mixture of 4-OH coumarin (5 mmol) and aromatic aldehyde (2.5 mmol) with 30 mg of catalyst in H_2O: EtOH were taken in a round bottom flask equipped with a magnetic stirrer. The mixture was stirred at 80 °C for an adequate time. The progress of the reaction was monitored by TLC. Dichloromethane was added to recover the catalyst. The acquired solid was dried and washed with ethanol to remove impurities. The desired products (**3a–j**) were obtained in high to excellent yields in a short period of time (10–25 min). The recovered catalyst was dried in an oven and again used for the next reaction.

Methodology of molecular docking

Molecular docking calculations were performed by using FlexX module[69,70] of LeadIT 2.1.8 program.[71] This module utilizes an incremental construction based algorithm[69] to assemble the ligand incrementally within the active site of the protein chain. Thus, it provides flexibility to the molecules selected for conducting docking. Moreover, this module calculates free binding energy (ΔG) of the docked ligand-protein complexes by employing the modified Böhm's scoring function.[72] In order to perform the molecular docking studies, 10 synthesized biscoumarin compounds (**3a–j**) were selected (Fig. 13).

These molecules were generated in the form of the SYBYL mol2 file format[73] and were compiled as a hit library. The constructed hit library was prepared in the Accelrys discovery studio version 4.0[74] which involved correction of the atoms, bond types, add hydrogen atoms, assign formal charges, and uses CHARMm force field[75] to minimize the energy of the ligands. The selected protein files of 4D75 and 6FCX were prepared in the Receptor Preparation Wizard of the FlexX[69,70] module of LeadIT 2.1.8 program.[71] The preparation involved the addition of the polar hydrogen atoms, assigning of the atom-type, and removal of the crystallographic water. The active site in the case of 4D75 was selected based on the known experimental inhibitor (PK9) with a defined radius of 6.5 Å around the inhibitor. However, in the case of 6FCX, the FlexX[69,70] modules of LeadIT[71] automatically detect the binding site present in the protein. Therefore, all the binding sites were docked separately in order to analyze the interaction pattern. The chemical uncertainties were resolved by employing ProToss module[76] of the LeadIT 2.1.8 program which optimized the ligands, cofactors, residues, and assigned the appropriate protonation and tautomers state within the binding site of the protein chain. In addition, to handle the steric clashes, default docking and chemical parameters were used. To perform the calculations, a hybrid entropy and enthalpy-based docking scheme were executed to locate the fragments. To find rational docking poses, the maximum number of solutions per interaction was set to 50. After docking, the docked interactions were reported in the form of protein-ligand 2D interaction plots via PoseView widget[77] of LeadIT 2.1.8 program.[71]

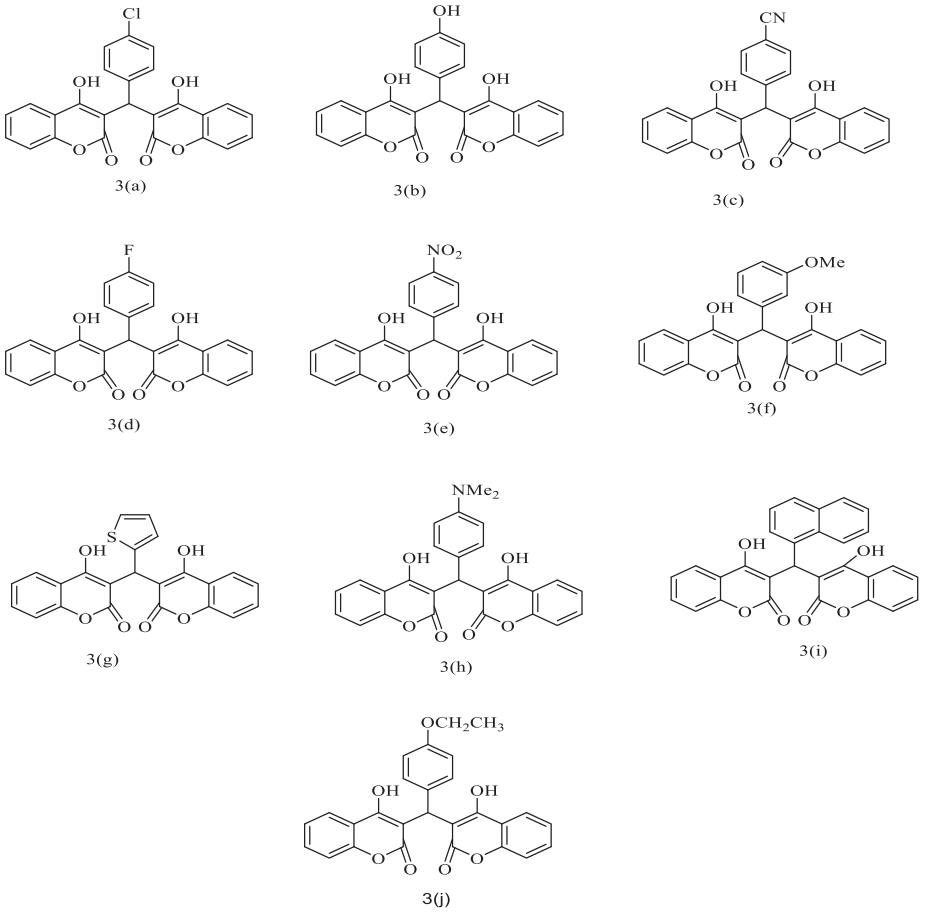

Figure 13. Library of synthesized Biscoumarin derivatives.

Table 8. Recyclability of Carbon-SO_3H catalyst for the synthesis of 4-Cl benzaldehdye.

Catalyst cycle	Fresh	I	II	III	IV	V	VI
Time (min)	20	20	20	20	25	25	25
Isolated yield (%)	100	100	99	96	90	86	80

Screening and reusability of the catalyst

The catalyst was insoluble in the reaction mixture and was recovered using dichloromethane (DCM). The recovered catalyst was washed with ethanol and dried in an oven for further use. The catalyst was recovered and reused up to the 5th run. For the first three runs, there is no loss in catalytic activity but for the next fourth run, there was slight decrease in the yield of the product. IR spectra showed that there is no change in the structure of recycled catalyst up to 3 runs. After the 5th run, the reaction time increased and the yield decreased (Table 8 and Fig. 14). The catalytic activity of recycled catalyst (Run 1, 2, and 3) can also be deduced by comparing its IR with a fresh catalyst (Fig. 15).

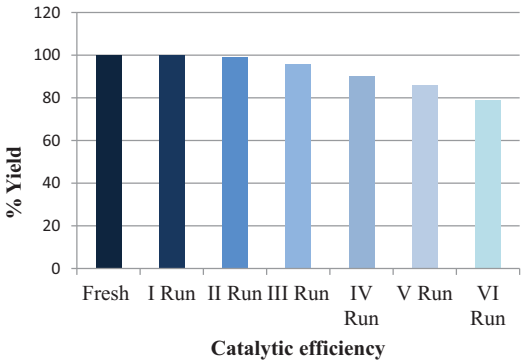

Figure 14. The catalytic efficiency of recovered catalyst.

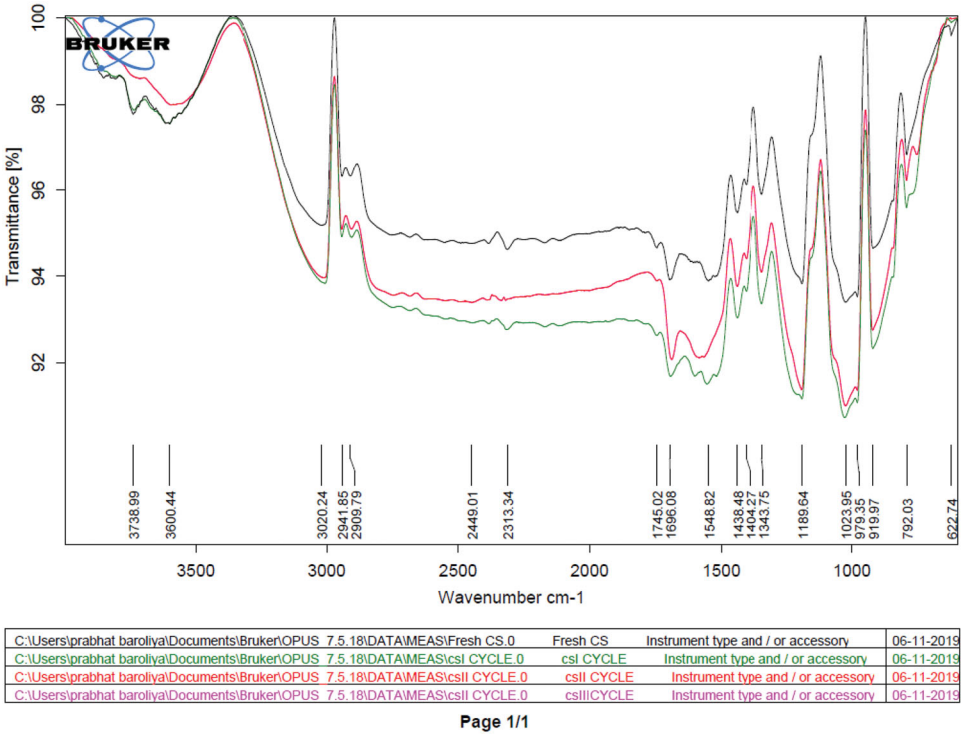

Figure 15. The IR spectrum of recovered catalyst with the fresh catalyst.

Spectral Characterization of synthesized biscoumarin derivatives

3,3′-((4-Chlorophenyl)methylene)-bis-(4-hydroxy-2H-chromen-2-one) (3a)

White solid; 100% Yield; mp 252–254 °C. (Lit. mp 258–260 °C)[26] IR max/cm^{-1} 3225–3058 (OH), 2919 (sp^3 C-H), 1671(C=O), 1600, 1511, 1493 (C=C aromatic), 1330 and 1091 (C–O), 746–935 (sp^2 C–H), 811–832 (Cl); ^{1}H NMR (500 MHz, DMSO-d_6) δ 6.31 (s, 1H, CH), 7.18 (dd, 2H, $J = 8.5$ Hz, 1 Hz, Ar–H), 7.27 (m, 2H, Ar–H), 7.30–7.33 (m, 2H Ar–H), 7.57–7.60 (m, 2H Ar–H), 7.89 (dd, $J = 8$ Hz, 1.5 Hz, 2H), 10.55 (broad,

2H, OH); ^{13}C NMR (100 MHz, DMSO-d_6) δ 165.13, 164.39, 155.39, 153.05, 133.08, 129.8, 128.66, 125.89, 124.75, 116.34, 114.99, 113.97, 103.58, 54.63, 34.22. ESI-MS (m/z): 446.5 (M+)

Full experimental details and copies of FT-IR, ^{1}HNMR spectra of all the synthesized compounds associated with this article have been provided in supporting information. The 2D and 3D docked structures of all the other derivatives with 6FCX and 4D75 protein, green chemistry matrix calculation, and eco-score are shown in the supplementary file. This material can be found via the "Supplementary Content" section of this article's webpage.

The experimental section of this work has been given in the supporting information. The ^{1}H NMR and IR spectrum of synthesized model compounds (**3a–j**) are provided. The 2D and 3D molecular docked structure of synthesized compounds is also provided in supporting information.

Acknowledgments

The authors are thankful to the Head of Department of Chemistry for providing necessary laboratory facilities. The Department of Physics, University College of science, MLSU, Udaipur is duly acknowledged for TGA, DTA, and XRD analysis. The authors would also like to acknowledge the Sophisticated Analytical Instrumentation Facility, Chandigarh, India, and Material Research Center Malviya National Institute of Technology Jaipur (MNIT, Jaipur) for carrying out the spectral analysis. A. Sethiya is thankful to UGC-MANF (MANF-2018-19-RAJ-91971) and P. Teli and N. Sahiba are thankful to CSIR for providing Junior Research Fellowship to carry out this work.

Funding

This work was supported by the UGC-MANF [MANF-2018-19-RAJ-91971] and CSIR.

References

[1] Bryan, M. C.; Dunn, P. J.; Entwistle, D.; Gallou, F.; Koenig, S. G.; Hayler, J. D.; Hickey, M. R.; Hughes, S.; Kopach, M. E.; Moine, G.; et al. *Green Chem.* **2018**, *20*, 5082–5103. DOI: 10.1039/C8GC01276H.

[2] Ehlers, D.; Pfister, M.; Gerard, D.; Quirin, K. W.; Bork, W. R.; Nadolny, P. T. *Int. J. Food Sci. Tech.* **1996**, *31*, 91–95. DOI: 10.1111/j.1365-2621.1996.19-319.x.

[3] Manolov, I.; Maichle-Moessmer, C.; Nicolova, I.; Danchev, N. *Arch. Pharm.* **2006**, *339*, 319–326. DOI: 10.1002/ardp.200500149.

[4] Abid, O.-U.-R.; Babar, T. M.; Ali, F. I.; Ahmed, S.; Wadood, A.; Rama, N. H.; Uddin, R.; Ul-Haq, Z.; Khan, A.; Choudhary, M. I. *ACS Med. Chem. Lett.* **2010**, *1*, 145. DOI: 10.1021/ml100068u.

[5] Ibrar, A.; Zaib, S.; Khan, I.; Jabeen, F.; Iqbal, J.; Saeed, A. *RSC Adv.* **2015**, *5*, 89919–89931. DOI: 10.1039/C5RA14900B.

[6] Asgari, M. S.; Mohammadi-Khanaposhtani, M.; Kiani, M.; Ranjbar, P. R.; Zabihi, E.; Pourbagher, R.; Rahimi, R.; Faramarzi, M. A.; Biglar, M.; Larijani, B.; et al. *Bioorg. Chem.* **2019**, *92*, 103206. DOI: 10.1016/j.bioorg.2019.103206.

[7] Li, J.; Meng, J. R.; Qu, D.; Zhang, Z.-D.; Li, F.; Yang, X. H.; Luo, X.-X.; Li, J.-T.; Li, M.-K. *Res. Chem. Intermed.* **2015**, *41*, 8257–8267. DOI: 10.1007/s11164-014-1889-x.

[8] Faisal, M.; Saeed, A.; Shahzad, D.; Fattah, T. A.; Lal, B.; Channar, P. A.; Mahar, J.; Saeed, S.; Mahesar, P. A.; Larik, F. A. *Eur. J. Med. Chem.* **2017**, *141*, 386–403. DOI: 10.1016/j.ejmech.2017.10.009.
[9] Su, C.-X.; Mouscadet, J.-F.; Chiang, C.-C.; Tsai, H.-J.; Hsu, L.-Y. *Chem. Pharm. Bull.* **2006**, *54*, 682–686. DOI: 10.1248/cpb.54.682.
[10] Perumalsamy, H.; Sankarapandian, K.; Veerappan, K.; Natarajan, S.; Kandaswamy, N.; Thangavelu, L.; Balusamy, S. R. *Phytomedicine* **2018**, *46*, 119–130. DOI: 10.1016/j.phymed.2018.04.021.
[11] Samija, M.; Elma, V.; Amar, O.; Jasmina, E.; Haris, N.; Hurija, D.; Davorka, Z. *IFMBE Proceedings*; Springer: Singapore, 2017.
[12] Mayank, A.; Singh, N.; Kaur, N.; Garg, N.; Singh, N. *Comput. Bio. Chem.* **2019**, *83*, 107104. DOI: 10.1016/j.compbiolchem.2019.107104.
[13] Zhang, H.; Luo, Q.; Mao, Y.; Zhao, Y.; Yu, T. *J. Photochem. Photobiol. A Chem.* **2017**, *346*, 10–16. DOI: 10.1016/j.jphotochem.2017.05.039.
[14] Narendran, K.; Nanthini, R. *New J. Chem.* **2015**, *39*, 4948–4956. DOI: 10.1039/C5NJ00322A.
[15] Pramod, A. G.; Nadaf, Y. F.; Renuka, C. G.; Sucheta, M. Biscoumarin derivative for designing the WLED display applications. *AIP Conference Proceedings 2115*, Hisar, Haryana, India, July 12, 2019. https://doi.org/10.1063/1.5113045.
[16] Marek, K.; Cławski, W.; Jakěsoѵ Charyton, M. M.; Demitri, N.; Koszarna, B.; Oppelt, K.; Sariciftci, S.; Gryko, D. T.; Głowacki, E. D. *J. Mater. Chem. A.* **2017**, *5*, 20780–20788. DOI: 10.1039/C7TA05882A.
[17] Rahmani, S.; Zeynizadeh, B. *Res. Chem. Intermed.* **2019**, *45*, 1227–1248. DOI: 10.1007/s11164-018-3671-y.
[18] Gandhi, D.; Agarwal, S. *J. Heterocyclic Chem.* **2018**, *55*, 2977–2984. DOI: 10.1002/jhet.3384.
[19] Agarwal, S.; Agarwal, D. K.; Gandhi, D.; Goyal, K.; Goyal, P. *Lett. Org. Chem.* **2018**, *15*, 863–869. DOI: 10.2174/1570178615666180326161710.
[20] Shahzad, D.; Saeed, A.; Faisal, M.; Larik, F. A.; Bilquees, S.; Channar, P. A. *Org. Prep. Proced. Int.* **2019**, *51*, 199–239. DOI: 10.1080/00304948.2019.1599788.
[21] Mahmoodi, N. O.; Pirbasti, F. G.; Jalalifar, Z. *J. Chin. Chem. Soc.* **2018**, *65*, 383–394. DOI: 10.1002/jccs.201700363.
[22] Abramovitch, R. A.; Gear, J. R. *Can. J. Chem.* **1958**, *36*, 151–1510. DOI: 10.1139/v58-019.
[23] Shirini, F.; Abedini, M.; Zamani, S.; Moafi, H. F. *J. Nanostruct. Chem.* **2015**, *5*, 123–130. DOI: 10.1007/s40097-014-0143-9.
[24] Abbasi, F.; Azizi, N.; Abdoli-Senejani, M. *J. Iran. Chem. Soc.* **2017**, *14*, 2097–2103. DOI: 10.1007/s13738-017-1146-5.
[25] Yang, C.; Su, W. Q.; Xu, D. Z. *RSC Adv.* **2016**, *6*, 99656–99663. DOI: 10.1039/C6RA23018K.
[26] Kauthale, S. S.; Tekale, S. U.; Jadhav, K. M.; Pawar, R. P. *Mol. Divers.* **2016**, *20*, 763–770. DOI: 10.1007/s11030-016-9673-z.
[27] Maleki, B. *Org. Prep. Proced. Int.* **2016**, *48*, 303–318. DOI: 10.1080/00304948.2016.1165061.
[28] Mayank, M.; Singh, A.; Raj, P.; Kaur, R.; Singh, A.; Kaur, N.; Singh, N. *New J. Chem.* **2017**, *41*, 3872–3881. DOI: 10.1039/C6NJ03763A.
[29] Safaei-Ghomi, J.; Eshteghal, F.; Shahbazi-Alavi, H. *Polycyclic Aromat. Compd.* **2017**, *40*, 13–20. doi.org/ DOI: 10.1080/10406638.2017.1348368..
[30] Azizi, N.; Abbasi, F.; Abdoli-Senejani, M. *Chem. Sel.* **2018**, *3*, 3797–3802. DOI: 10.1002/slct.201800138.
[31] Brahmachari, G.; Begam, S. *Chem. Sel.* **2019**, *4*, 5414.
[32] Daneshvar, N.; Goli-Jolodar, O.; Karimi-Chayjani, R.; Langarudi, M. S. N.; Shirini, F. Sustainable and Eco-Friendly Method for the Synthesis of Some Bioactive Derivatives of Biscoumarin and Pyrano[3,2-c]Chromene-3-Carbonitrile Using Taurine, as the Catalyst. *Chem. Sel.* **2019**, *4*, 1562–1566. DOI: 10.1002/slct.201803210.

[33] Faisal, M.; Larik, F. A.; Saeed, A. *J. Porous* Mater. **2019**, *26*, 455–466. DOI: 10.1007/s10934-018-0625-0.
[34] Mathavan, S.; Kannan, K.; Yamajal, R. B. R. D. *Org. Biomol. Chem.* **2019**, *17*, 9620–9626. DOI: 10.1039/c9ob02090j.
[35] Zhu, A.; Bai, S.; Li, L.; Wang, M.; Wang, J. *Catal. Lett.* **2015**, *145*, 1089–1093. DOI: 10.1007/s10562-015-1487-6.
[36] Hamdi, N.; Puerta, M. C.; Valerga, P. *Eur. J. Med. Chem.* **2008**, *43*, 2541–2548. DOI: 10.1016/j.ejmech.2008.03.038.
[37] Singh, P.; Kumar, P.; Katyal, A.; Kalra, R.; Dass, S. K.; Prakash, S.; Chandra, R. *Catal. Lett.* **2010**, *134*, 303–308. DOI: 10.1007/s10562-009-0239-x.
[38] Montazeri, N.; Vahabi, V. *Bulg. Chem. Commun.* **2015**, *47*, 136.
[39] Kiasat, A. R.; Hemat-Alian, L. *Res. Chem. Intermed.* **2015**, *41*, 873–880. DOI: 10.1007/s11164-013-1239-4.
[40] Shirini, F.; Khaligh, N. G. *Chin. J. Catal.* **2013**, *34*, 1890–1896. DOI: 10.1016/S1872-2067(12)60669-X.
[41] Tabatabaeian, K.; Heidari, H.; Khorshidi, A.; Mamaghani, M.; Mahmoodi, N. O. *J. Serb. Chem. Soc.* **2012**, *77*, 407–413. DOI: 10.2298/JSC110427189T.
[42] Vahabi, V.; Hatamjafari, F. *Orient. J. Chem.* **2014**, *30*, 853–855. DOI: 10.13005/ojc/300263.
[43] Seddighi, M.; Shirini, F.; Mamaghani, M. *RSC Adv.* **2013**, *3*, 24046. DOI: 10.1039/c3ra44053b.
[44] Rezaei, R.; Sheikhi, M. R. *Res. Chem. Intermed.* **2015**, *41*, 1283–1292. DOI: 10.1007/s11164-013-1272-3.
[45] Niknama, K.; Sajadi, S. A.; Hosseini, R.; Baghernejad M. *Iran. J. Catal.* **2014**, *4*, 163.
[46] Sedighi, M.; Montazeri, N. *Adv. Stud. Biol.* **2015**, *7*, 89–95. DOI: 10.12988/asb.2015.41160.
[47] Iravani, N.; Keshavarz, M.; Mousavi, M.; Baghernejad, M. *Iran. J. Catal.* **2015**, *5*, 65.
[48] Ghorbani, F.; Pourmousavi, S. A.; Kiyani, H. *Curr. Organocat.* **2019**, *7*, 55–80. DOI: 10.2174/2213337206666190717164606.
[49] Teli, P.; Sethiya, A.; Agarwal, S. An Insight View on Synthetic Protocol, Mechanistic and Biological Aspects of Biscoumarin Derivatives. *Chem. Sel.* **2019**, *4*, 13772–13787. DOI: 10.1002/slct.201903632.
[50] Karnakar, K.; Murthy, S. N.; Kumar, R.; Nageswar, Y. V. D.; Reddy, T. V. K.; Bethala, B. L. A.; Devi, P.; Prasad, R. B. N. *Tetrahedron Lett.* **2012**, *53*, 1968.
[51] Ramesh, R.; Sankar, G.; Malecki, J. G.; Appaswami, L. *J. Iran. Chem. Soc.* **2018**, *15*, 1–9. DOI: 10.1007/s13738-017-1202-1.
[52] Zhang, H.; Wang, W.; Zhang, B.; Li, H.; Zhang, Q. *RSC Adv.* **2016**, *6*, 30956–30962. DOI: 10.1039/C6RA01680D.
[53] Karnakar, K.; Murthy, S. N.; Ramesh, K.; Reddy, K. H. V.; Nageswar, Y. V. D.; Chandrakala, U.; Devi, B. L. A. P.; Prasad, R. B. N. *Tetrahedron Lett.* **2012**, *53*, 3497–3501. DOI: 10.1016/j.tetlet.2012.04.122.
[54] Singh, R.; Ganaie, S. A.; Singh, A.; Chaudhary, A. *Synth. Commun.* **2019**, *49*, 80–93. DOI: 10.1080/00397911.2018.1542003.
[55] Avdović, E. H.; Milenković, D.; Marković, J. M.; Đorović, J.; Vuković, N.; Vukić, M. D.; Jevtić, V. V.; Trifunović, S. R.; Potočňák, I.; Marković, Z. *Spectrochim Acta A Mol Biomol Spectrosc.* **2018**, *195*, 31–40. DOI: 10.1016/j.saa.2018.01.023.
[56] Kaur, P.; Chamberlin, A. R.; Poulos, T. L.; Sevrioukova, I. F. *J. Med. Chem.* **2016**, *59*, 4210–4220. DOI: 10.1021/acs.jmedchem.5b01146.
[57] Froese, D. S.; Kopec, J.; Rembeza, E.; Bezerra, G. A.; Oberholzer, A. E.; Suormala, T.; Lutz, S.; Chalk, R.; Borkowska, O.; Baumgartner, M. R.; et al. *Nat. Commun.* **2018**, *9*, 2261. DOI: 10.1038/s41467-018-04735-2.
[58] Xu, L.; Liu, H.; Murray, B. P.; Callebaut, C.; Lee, M. S.; Hong, A.; Strickley, R. G.; Tsai, L. K.; Stray, K. M.; Wang, Y.; et al. *ACS Med. Chem. Lett.* **2010**, *1*, 209–213. DOI: 10.1021/ml1000257.
[59] Stankova, J.; Lawrance, A.; Rozen, R. *Curr. Pharm. Des.* **2008**, *14*, 1143–1150. DOI: 10.2174/138161208784246171.

[60] Devi, B. L. A. P.; Gangadhar, K. N.; Prasad, P. S. S.; Jagannadh, B.; Prasad, R. B. N. *ChemSusChem.* **2009**, *2*, 617–620. DOI: 10.1002/cssc.200900097.
[61] Devi, B. L. A. P.; Gangadhar, K. N.; Siva Kumar, K. L. N.; Shiva Shanker, K.; Prasad, R. B. N.; Sai Prasad, P. S. *J. Mol. Catal. A. Chem.* **2011**, *345*, 96–100. DOI: 10.1016/j.molcata.2011.05.025.
[62] Estes, C. S.; Gerard, A. Y.; Godward, J. D.; Hayes, S. B.; Liles, S. H.; Shelton, J. L.; Stewart, T. S.; Webster, R. I.; Webster, H. F. *Carbon*. **2019**, *142*, 547–557. DOI: 10.1016/j.carbon.2018.10.074.
[63] Kong, P. S.; Aroua, M. K.; Daud, W. M. A. W.; Lee, H. V.; Cognet, P.; Peres, Y. *RSC Adv.* **2016**, *6*, 68885–68905. DOI: 10.1039/C6RA10686B.
[64] Liu, F.; Sun, J.; Zhu, L.; Meng, X.; Qi, C.; Xiao, F.-S. *J. Mater. Chem.* **2012**, *22*, 5495. DOI: 10.1039/c2jm16608a.
[65] Lee, D. *Molecules* **2013**, *18*, 8168–8180. DOI: 10.3390/molecules18078168.
[66] Gong, G.-X.; Zhou, J.-F.; An, L.-T.; Duan, X.-L.; Ji, S.-J. *Synth. Commun.* **2009**, *39*, 497–505. DOI: 10.1080/00397910802398272.
[67] Constable, D. J.; Curzons, A. D.; Cunningham, V. L. *Green Chem.* **2002**, *4*, 521–527. DOI: 10.1039/B206169B.
[68] Bahuguna, A.; Kumar, S.; Sharma, V.; Reddy, K. L.; Bhattacharyya, K.; Kumar, P. C. R.; Krishnan, V. *ACS Sustainable Chem. Eng.* **2017**, *5*, 8551–8567. DOI: 10.1021/acssuschemeng.7b00648.
[69] Rarey, M.; Kramer, B.; Lengauer, T.; Klebe, G. *J. Mol. Biol.* **1996**, *261*, 470–489. DOI: 10.1006/jmbi.1996.0477.
[70] Kramer, B.; Rarey, M.; Lengauer, T. *Proteins* **1997**, *29*, 221–225. DOI: 10.1002/(SICI)1097-0134(1997)1+<221::AID-PROT30>3.0.CO;2-O.
[71] *LeadIt*, version 2.1.8, BioSolveIT GmbH. BioSolveIT: Sankt Augustin, Germany.
[72] Böhm, H.-J. *J. Comput. Aided Mol. Des.* **1994**, *8*, 243–256. DOI: 10.1007/BF00126743.
[73] *SYBYL*, TRIPOS Associates Inc.: St. Louis, MO, 1994.
[74] *Discovery Studio*, version 4.0, Accelrys Software, Inc.: San Diego, CA, www.accelrys.com/products/collaborativescience/biovia-discovery-studio/
[75] Brooks, B. R.; Bruccoleri, R. E.; Olafson, B. D.; States, D. J.; Swaminathan, S. A.; Karplus, M. *J. Comput. Chem.* **1983**, *4*, 187–217. DOI: 10.1002/jcc.540040211.
[76] Bietz, S.; Urbaczek, S.; Schulz, B.; Rarey, M. *J. Cheminform.* **2014**, *6*, 12. DOI: 10.1186/1758-2946-6-12.
[77] Stierand, K.; Rarey, M. *ACS Med. Chem. Lett.* **2010**, *1*, 540–545. DOI: 10.1021/ml100164p.